A Low-Computational High-Performance Model Predictive Control of Single Phase Battery Assisted Quasi Z-Source PV Inverters

Lashab, Abderezak; Séra, Dezso; Guerrero, Josep M.

Published in:
Proceedings of 2019 10th International Conference on Power Electronics and ECCE Asia (ICPE 2019 - ECCE Asia)

Publication date:
2019

Document Version
Accepted author manuscript, peer reviewed version

A Low-Computational High-Performance Model Predictive Control of Single Phase Battery Assisted Quasi Z-Source PV Inverters

Abderezak Lashab, Dezso Sera, Josep M. Guerrero
Department of Energy Technology, Aalborg University, Aalborg DK-9220, Denmark
abl@et.aau.dk, des@et.aau.dk, joz@et.aau.dk

Abstract—**Impedance network inverters are a good alternative for voltage-source and current-source inverters. The shoot-through solution and the boosting capability of such converters make them an excellent solution for photovoltaic (PV) application. Furthermore, energy storage integration in these inverters does not require any additional components in the converter; indeed, a battery can be directly connected in parallel with one of the capacitors of the Z- or quasi Z-network. However, for an optimal control of these converters, complex control and modulation strategies are required. Model Predictive Control (MPC) provides high control performance at the expense of the computational effort. In this paper, a low computational control method where both MPC and proportional resonant (PR) controller are combined, is proposed. This makes the proposed controller perform two iterations only instead of iterating for all the available switching states. As shown in the obtained results, the proposed controller conserves the high performance of the conventional MPC with 50% less computational burden.**

Keywords—**Computational effort, Battery, Feedforward, Grid connected, Modular, MPC, MPPT, Photovoltaic, P&O, Z-network.**

I. INTRODUCTION

Because of environmental issues as well as economic considerations, there is an upward tendency in developing the use of solar energy [1]. Therefore, there is an ascending demand for grid-connected and stand-alone photovoltaic (PV) power generation systems. With this growth, intense development of power electronics converters and their control have been done [2], [3].

The most well known converters are the voltage source converter (VSC) and the current source converter (CSC), due to their wide applicability in various applications [4], [5], [6]. A VSC that switches a dc voltage source is able to provide a less voltage level at the output only. However, this is considered a critical issue in PV systems, since the PV arrays provide power with a low voltage level, and boosting it is a must. When using VSCs in PV systems, usually a dc-dc boost converter is used to boost the voltage before the inversion stage [7]. Another alternative consists of installing a transformer at the output of the inverter [8]. The aforementioned two solutions suffer from decreased efficiency since the conversion system is double staged.

Z-source (ZS) and quasi Z-source inverters (qZSI) have been broadly investigated since they are able to cope with the boosting issue [9], [10], [11]. In addition, a previous comparison between the classical two-stage inverter and the qZSI in [12] and [13] indicated that the qZSI uses smaller passive components and less active switches; hence, it can be implemented with a lower cost. In terms of efficiency, qZSIs reach almost the same or higher [12].

The power generated from solar panels is intermittent and has stochastic characteristics [14]. According to the updated grid codes, the change of power injected to the grid is limited, which requires energy storage in order to limit the power change [15]. Conventionally, in order to install a battery in a PV system, a bidirectional converter is needed, which is usually paralleled to the dc-link capacitor of a dual power conversion stage PV system [16]. Among the advantages of ZS- and qZS inverters is their unique structure that allows battery integration without any extra element in the circuit, resulting in a cheap and less sizable solution [17], [18].

MPC is an intuitive and powerful tool that has been a direction of many researchers [19]-[20]. In power electronics, finite-control-set (FCS) is the most adopted class of MPC since it is simple, includes nonlinearities and constrains, and robust [21]. FCS-MPC predicts the behavior of the controlled variables based on the model of the system as function of the possible switching states. Hence, the prediction is performed k times in each sampling time, assuming that k is the total number of the available switching states. These predictions are then compared to the provided reference through the cost function, and the switching state that corresponds to the minimized cost function is chosen to be applied during the next sampling time [23]-[26]. Although the operation principle of FCS-MPC is not complex, a high computational effort is needed, especially in some application where the power converter has a high number of possible switching states, such as modular multilevel converters (MMC).

In this paper, the control algorithm is a combination of FCS-MPC and PR controller. The grid current is controlled through a PR controller, whereas the qZ network variables, such as the PV current and battery current are controlled through FCS-MPC. Hence, the prediction in FCS is shortened to two states only, zero state and shoot through state. Accordingly, the outcome of the proposed idea is a mitigated double line-frequency ripple in the battery current with a reduced computational burden.

II. The Configuration of the Single Phase Energy Stored Quasi Z-source Inverter

The configuration of the single phase qZSI for PV systems with integrated battery is shown in Fig. 1. The single phase qZSI consists of two parts, qZ network and an H-bridge. The qZ network is where the power sources are connected, and is composed of two capacitors, two inductors, and a diode. The PV is connected to the input of the converter, and the battery can be connected in parallel with one of the capacitors of the qZ network. In this paper, the battery is paralleled to the second capacitor of the Z-network C_2, since it operates with lower voltage. In qZS inverters, a shoot through state is also added during the zero state. The equivalent circuits of the single phase qZSI during the active, zero, and shoot through states are shown in Fig. 2(a), Fig. 2(b), and Fig. 2(c), respectively.

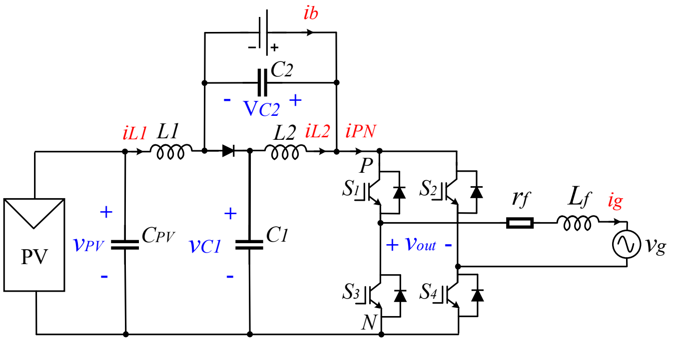

Fig. 1. Single phase battery assisted Quasi Z-source inverter for PV systems.

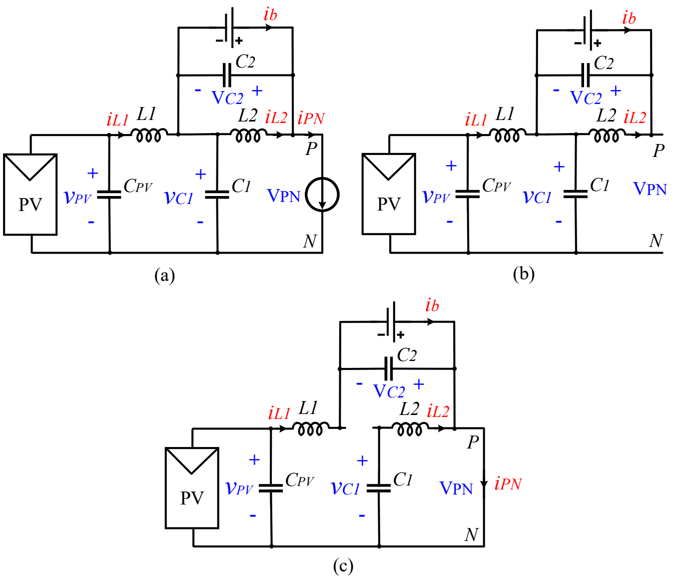

Fig. 2. The equivalent circuit of single phase battery assisted Quasi Z-source inverter for PV systems during: (a) active states; (b) zero state, and (c) shoot through state.

III. Conventional Finite Control Set-MPC Applied to Single Phase Energy Stored Quasi Z-source Inverter

A. ac side control of the quasi Z-source inverter,

According to Fig. 1, and based on Kirchhoff's voltage law, the output voltage of the single phase qZSI can be accessed as follows:

$$v_{out}(t+T_s) = v_{PN}(S_1 - S_2) \tag{1}$$

where v_{PN} is the voltage at the input of the H-bridge, S_1 and S_2 are the upper switches states. The output voltage as function of the current injected to the grid and filter inductance and stray resistance can be found similarly as the following:

$$v_{out} = L_f \frac{di_g}{dt} + r_f i_g + v_g \tag{2}$$

where L_f, r_f, i_g, and v_g are the filter inductance, filter stray resistance, the grid current, and the grid voltage, respectively. The most used approach for the discretization is Euler's forward law,

$$\frac{d\,x(t)}{dt} \approx \frac{x(t+T_s) - x(t)}{T_s} \tag{3}$$

such as, T_s is the discretization sampling time. By merging Euler's law into (2), the predicted grids current can be found as:

$$i_g(t+T_s) = i_g(t) + \frac{T_s}{L_f}\left(v_{out}(t+T_s) - r_f i_g(t) - v_g(t)\right) \tag{4}$$

B. dc side control of the quasi Z-source inverter,

1) active states

By applying Kirchhoff's voltage law on Fig. 2(a), the inductor voltages can be obtained as:

$$\begin{cases} L_1 \dfrac{di_{L1}}{dt} = v_{pv} - i_{L1} r_{L1} - v_{C1} \\ L_2 \dfrac{di_{L2}}{dt} = -i_{L2} r_{L2} - v_{C2} \\ C_1 \dfrac{dv_{C1}}{dt} = i_{L1} - i_{PN} \\ C_2 \dfrac{dv_{C2}}{dt} = i_{L2} - i_{PN} + i_b \end{cases} \tag{5}$$

where i_{L1}, i_{L2}, v_{C1}, v_{C2}, r_{L1}, and r_{L2} are the current through inductor L_1, the current through inductor L_2, capacitor C_1 voltage, capacitor C_2 voltage, inductor L_1 internal resistance, and inductor L_1 internal resistance, respectively. The predicted inductor L_1 current and capacitor voltage can be assessed by discretizing their corresponding equations in (5).

By applying Euler's approximation on (5), the first inductor predicted current and first capacitor voltage can be found as:

$$i_{L1}(t+T_s) = i_{L1}(t) + \frac{T_s}{L_1}\left(v_{pv}(t) - i_{L1}(t) r_{L1} - v_{C1}(t)\right) \tag{6}$$

$$v_{C1}(t+T_s) = v_{C1}(t) + \frac{T_s}{C_1}\left(i_{L1}(t) - i_{PN}(t)\right) \tag{7}$$

The current through the battery is estimated as:

$$i_b = i_{L2} - i_{L1} \tag{8}$$

By substituting the inductors predicted currents into (8), the predicted current can be found as follows:

$$i_b(t+T_s) = i_{L2}(t) - \frac{T_s}{L_2} v_{C2} - i_{L1}(t+T_s) \tag{9}$$

2) Zero state

As it can be seen from Fig. 2(b), the inductors currents are the same as in the active states, whereas the capacitors voltages are as follows:

$$\begin{cases} C_1 \dfrac{dv_{C1}}{dt} = i_{L1} \\ C_2 \dfrac{dv_{C2}}{dt} = -i_{L2} \end{cases} \tag{10`}$$

Hence, the predicted first capacitor voltage can be expressed as:

$$v_{C1}(t+T_s) = v_{C1}(t) + \frac{T_s}{C_1} i_{L1}(t) \tag{11}$$

3) Shoot through state

From Fig. 2(c), the inductors currents and capacitors voltages can be found as:

$$\begin{cases} L_1 \dfrac{di_{L1}}{dt} = v_{pv} - i_{L1} r_{L1} + v_{C2} \\ L_2 \dfrac{di_{L2}}{dt} = -i_{L2} r_{L2} + v_{C1} \\ C_1 \dfrac{dv_{C1}}{dt} = -i_{L2} \\ C_2 \dfrac{dv_{C2}}{dt} = -i_{L1} + i_b \end{cases} \tag{12}$$

The application of Euler's method on (12) results in:

$$i_{L1}(t+T_s) = i_{L1}(t) + \frac{T_s}{L_1}\left(v_{pv}(t) - i_{L1}(t) r_{L1} + v_{C2}(t)\right) \tag{13}$$

$$v_{C1}(t+T_s) = v_{C1}(t) - \frac{T_s}{C_1} i_{L2}(t) \tag{14}$$

$$i_b(t+T_s) = i_{L2}(t) + \frac{T_s}{L_2} v_{C1} - i_{L1}(t+T_s) \tag{15}$$

In case of qZSI without battery, the voltage in one of the Z-network is controlled. But, since the second capacitor C_2 is in parallel with a battery, its voltage level is determined by the state of charge (SOC) of the battery. Hence, the battery current is controlled instead. In this case, the cost function has the following form:

$$g = \lambda_{ig} g_{ig} + \lambda_{PV} g_{PV} + \lambda_b g_b \tag{16}$$

where

$$g_{ig} = \left| i_g^{ref}(t+T_s) - i_g(t+T_s) \right|;$$

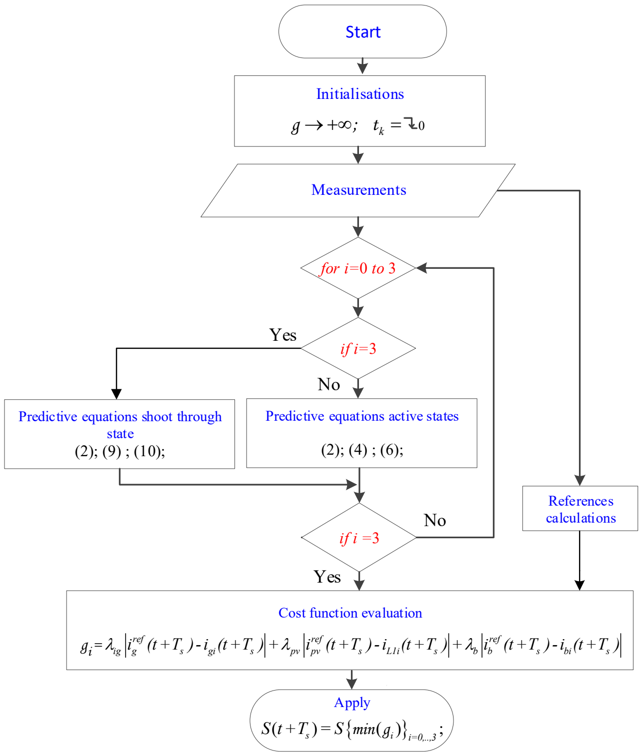

Fig. 3. Flowchart of the conventional FCS-MPC for the PV fed qZSI with integrated energy storage [23].

$$g_{PV} = \left| i_{pv}^{ref}(t+T_s) - i_{L1}(t+T_s) \right|;$$

$$g_b = \left| i_b^{ref}(t+T_s) - i_b(t+T_s) \right|$$

λ_{ig}, λ_{PV}, and λ_b are the weighting factors of the terms of the grid current, the PV current and, the battery current, respectively. $i_g^{ref}(t+Ts)$ is the desired grid current, $i_{PV}^{ref}(t+Ts)$ is PV current reference, which is provided by the maximum power point tracking (MPPT) algorithm, and $i_g^{ref}(t+Ts)$ is estimated as:

$$i_b^{ref} = \frac{P_b}{v_{C2}} \tag{17}$$

such as, P_b is the power absorbed/delivered by the battery, and is estimated as:

$$P_b = P^{ref} - P_{pv} \tag{18}$$

The MPPT adopted in this paper is the conventional Perturb and Observe (P&O) [22]. In order to calculate the predicted variables and the cost functions for a defined switching states, an algorithm should be designed. Fig. 3 shows a previously introduced FCS-MPC algorithm for qZSI [23].

IV. Proposed Finite-Control-Set MPC for the Energy Stored Single Phase Quasi Z-Source

The proposed control structure is composed of two parts, one part for the regulation of the grid current to the desired

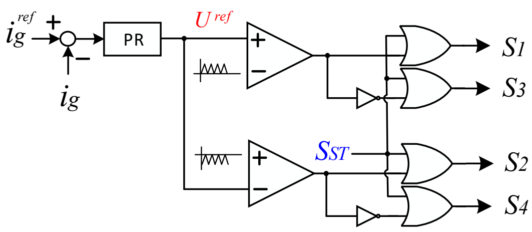

Fig. 4. Gird current regulation and switching state generation in the proposed controller.

one, and the second part is responsible for maintaining both the PV current to the reference provided by the MPPT and the battery current to its reference. Fig. 4 shows the grid current control and the modulation stage. The control of the PV and battery currents is summarized in Fig. 5. Since only the PV and battery currents are going to be controlled through MPC, the cost function contains two terms,

$$g = \lambda_{PV} g_{PV} + \lambda_b g_b \tag{19}$$

The prediction in the proposed control is done for two states only, zero state and shoot through state. Hence, the index j in Fig. 4 has two values "0" for zero state, and "1" for shoot through state. Similar to the conventional FCS-MPC, the inductor current is predicted based on (6) for the zero state and (13) for the shoot through state. The battery current is predicted by using (9) for the zero state and (15) for the shoot through

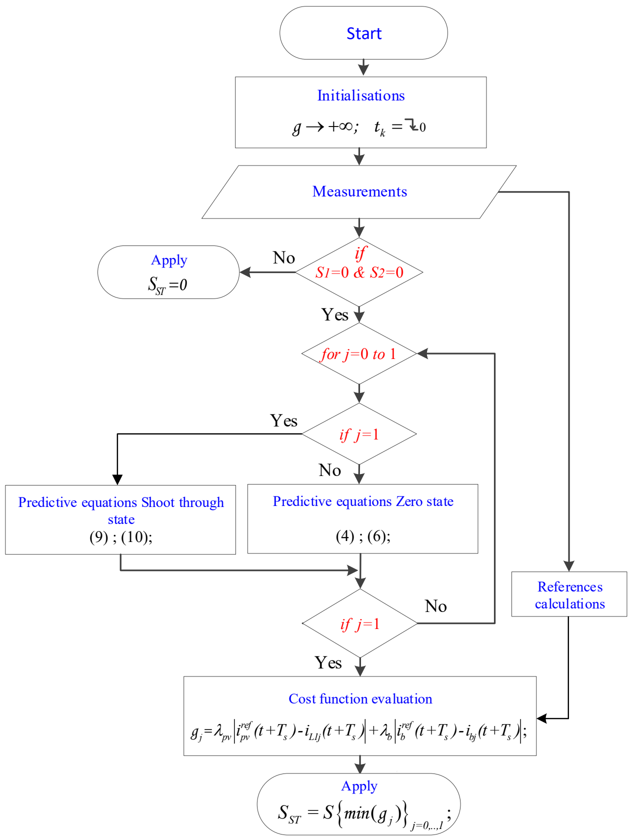

Fig. 5. Shoot through state generation in the proposed controller.

TABLE I.
A COMPARAISON OF THE PROPOSED CONTROLLER WITH FCS-MPC IN TERMS OF THE NUMBER OF MATHEMATICAL OPERATIONS

Method			+ & –	×	÷
FCS-MPC	*Per iteration*		*13*	*8*	*3*
	4 iterations		***52***	***32***	***12***
Proposed controller	*Prediction model*	*Per iteration*	*8*	*5*	*2*
		2 iterations	*16*	*10*	*4*
	PR		*8*	*13*	*1*
			24	***23***	***5***

state. The predicted variables are compared with their references through the cost function, and the switching state corresponding to the minimized cost function will be applied during the next sampling time. i.e. if the predicted variables corresponding to the shoot through state minimize the cost function, then a shoot through will be applied, a zero state will be applied otherwise. In this paper, the shoot through is decided as a high logic value through the output of the algorithm S_{ST} instead of a duty cycle. The controller runs the algorithm only if the current state is zero state (S_1=0 & S_2=0), in order to avoid the overlap with the control of the grid current.

Table I shows a comparison between FCS-MPC and the proposed controller in terms of the number of mathematical operations. FCS-MPC performs 12 additions and subtractions, 8 multiplications, and 3 divisions in each iteration. These numbers are multiplied by the total number of iterations, which equals to the number of the available switching states, 4. The proposed controller on the prediction model side performs 8 additions and subtractions, 5 multiplications, and 2 divisions in each of the two iterations, shoot through state iteration and zero state iteration. The PR controller executes 8 additions and subtractions, 13 multiplications, and 1 division, considering its discretization through the trapezoidal method [27]. The later method provides very good results when applied to PR controllers, compared to Euler's discretization. As it can be seen from the same table, the total number of mathematical operations required in the proposed MPC is around half of the one required by FCS-MPC.

V. SIMULATION RESULTS AND DISCUSSION

For validating the theoretical analysis, a 2-kw single phase qZSI inverter has been designed using the previously shown equations. The specification of the PV panels were taken from the back of a PV panel that is available the Lab (Universal Solar WXS230P-US). The PV panels parameters are shown in Table I. In order to reach a higher voltage in the dc-link than the grid one, ten PV panels were connected in series. The battery is a Lithium-ion type, its nominal voltage and capacity are 48V and 6Ah, respectively. The inverter and filter parameters are shown in Table. II.

TABLE II.
PV PANEL, UNIVERSAL SOLAR WXS230P-US

Parameter	Value
Maximum power, P_{MPP}	*230W*
Maximum power current, I_{MPP}	*7.52A*
Short circuit current, I_{sc}	*8.56A*
Open circuit voltage, v_{oc}	*36.9V*

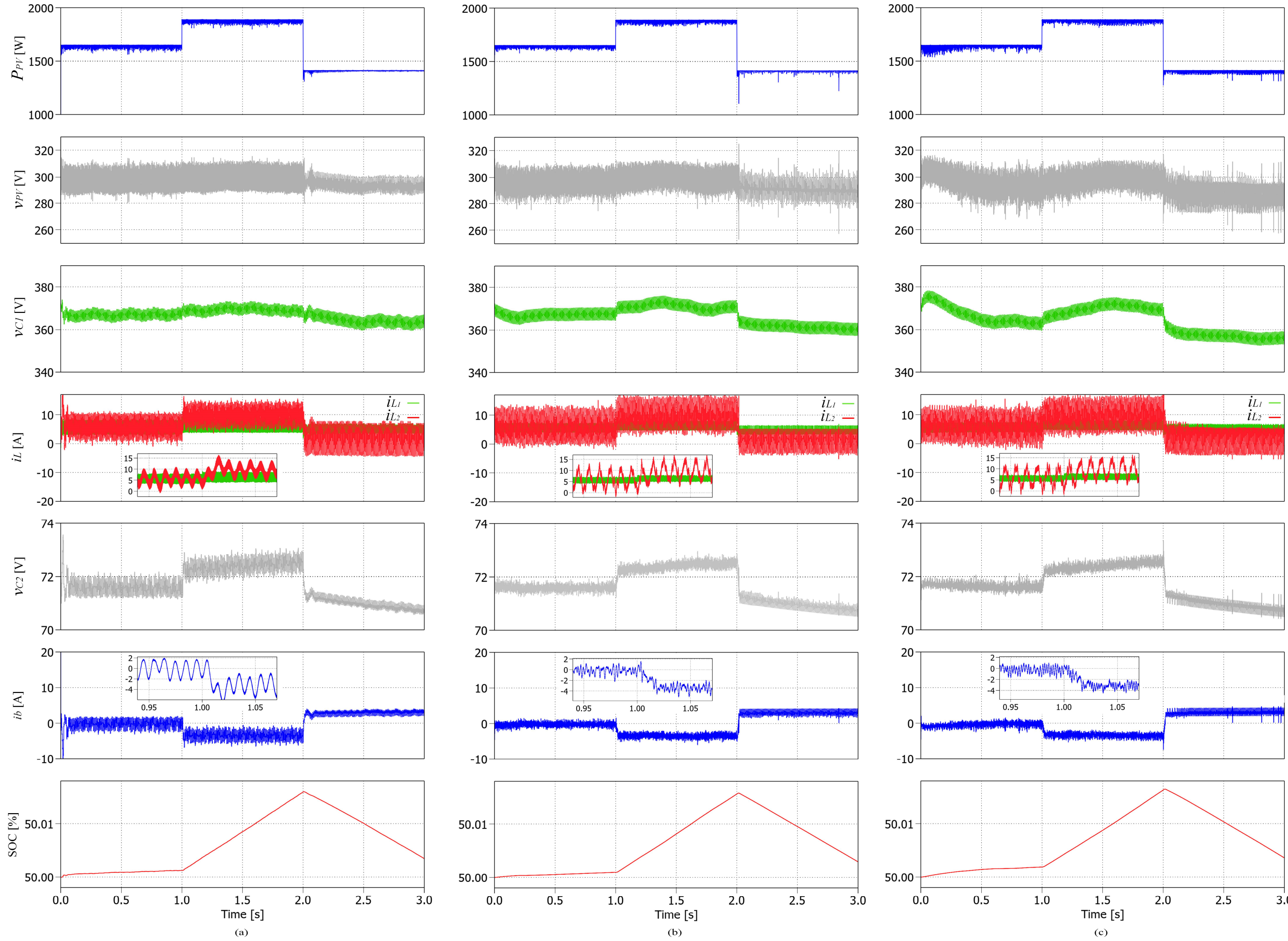

Fig. 6. Simulation results of the single phase qZSI for photovoltaic systems with integrated energy storage, tested using: (a) the linear PI controllers; (b) FCS-MPC; (c) the proposed MPC controller.

As assumed in the theoretical study, the inverter is going to be tested under different meteorological conditions. For comparison purposes, the results when the converter is operating by using the linear PI controllers are also included, and they are shown in Fig. 6(a). The results shown in Fig. 6 (b) are from the conventional FCS-MPC, whereas the ones shown in Fig. 6 (c) correspond to the proposed control scheme. The system started operating under an average solar irradiance, where the power generated by the PV arrays is just equal to the active power reference. The battery in this case float. After one second from the starting of the test, the irradiance increases to a point where the PV arrays generate a higher power than the power injected to the grid, thus, the battery converts to charging mode. At the third second of the test, the irradiance decreases, where the power generated by the PV arrays becomes insufficient for feeding the required power to the grid. The battery in this case swap from charging mode to discharging mode in order to compensate for the lack of power. As it can be seen from Fig. 6 (a), the conventional control based on linear PI controllers for the single phase qZSI with integrated energy storage suffers from a double line-frequency ripple in the battery current, which is measured as Δi_b=5.11A.

From Fig. 6 (b), it can be seen that the ripple in the battery current has been mitigated to Δi_b=2.52A, at the expenses of the second qZ network's inductor current i_{L2} and the first qZ network's capacitor voltage v_{C1} when the conventional FCS-MPC is applied. It can be seen from Fig. 6(c), that the proposed controller provides equivalent performance to the conventional FCS-MPC, with a battery current ripple equals to Δi_b=2.39A, although the computational burden has been reduced by around half.

TABLE III.
INVRTER AND FILTER SPECIFICATIONS

Parameter	Value
Filter inductance, L_f	*10mH*
Stray resistor of each inductance, R_L	*0.1Ohm*
Z-network inductors, $L_{1,2}$	*0.8mH*
Z-network capacitor C_1	*2000µF*
Z-network capacitor C_2	*800µF*
PV module capacitor, C_{pv}	*20µF*
Switching frequency, f_{sw}	*10KHz*

VI. CONCLUSION

A low computational control algorithm based on MPC for battery assisted single phase qZSI for PV systems has been proposed in this paper. Energy stored single phase qZS inverters suffer from a double line-frequency ripple in the battery current. This ripple can be mitigated by either increasing the size of the passive elements or by implementing advanced control strategies, such as MPC. However, MPC is computationally expensive considering that the algorithm has to iterate as the same number of the available switching states. The computational burden has been reduced by around 50% since the iterations required in the proposed control strategy are only two. The obtained simulation results confirmed that the proposed algorithm still conserves the high performance of the conventional FCS-MPC, seeing that the double line-frequency ripple in the battery current is equivalently reduced.

VII. REFERENCES

[1] H. Fathabadi, "Effect of External AC Electric and Magnetic Fields on the Power Production of a Silicon Solar Cell," *in IEEE Journal of Photovoltaics*, vol. 8, no. 6, pp. 1408-1412, Nov. 2018.

[2] B. J. Pierquet and D. J. Perreault, “A single-phase photovoltaic inverter topology with a series-connected energy buffer,” *IEEE Trans. Power Electron*., vol. 28, no. 10, pp. 4603–4611, Oct. 2013.

[3] Y. Tang, Y. Bai, J. Kan, and F. Xu, “Improved dual boost inverter with half cycle modulation,” *IEEE Trans. Power Electron*., vol. 32, no. 10, pp. 7543–7552, Oct. 2017.

[4] A. Yazdani and R. Iravani, Voltage-Sourced Converters in Power Systems:Modeling, Control, and Applications. New York, NY, USA: *Wiley*, 2010.

[5] H. F. Ahmed, H. Cha, S. H. Kim, and H. G. Kim, “Switched-coupledinductor quasi-z-source inverter,” *IEEE Trans. Power Electron.*, vol. 31, no. 2, pp. 1241–1254, Feb. 2016.

[6] V. Fern, A. Cordeiro, D. Foito, and J. F. Martins, “Quasi-z-source inverter with a t-type converter in normal and failure mode,” *IEEE Trans. Power Electron*., vol. 31, no. 11, pp. 7462–7470, Nov. 2016.

[7] A. Lashab, D. Sera, J. M. Guerrero, L. Mathe and A. Bouzid, "Discrete Model-Predictive-Control-Based Maximum Power Point Tracking for PV Systems: Overview and Evaluation," *in IEEE Trans. Power Electron.*, vol. 33, no. 8, pp. 7273-7287, Aug. 2018.

[8] V. N. Lal and S. N. Singh, "Control and Performance Analysis of a Single-Stage Utility-Scale Grid-Connected PV System," in IEEE Systems Journal, vol. 11, no. 3, pp. 1601-1611, Sept. 2017.

[9] B. Ge et al., “An energy stored quasi-Z-source inverter for application to photovoltaic power system,” *IEEE Trans. Ind. Electron*., vol. 60, no. 10, pp. 4468–4481, Oct. 2013.

[10] D. Sun, B. Ge, W. Liang, H. Abu-Rub, and F. Z. Peng, “An energy stored quasi-Z-source cascade multilevel inverter-based photovoltaic power generation system,” *IEEE Trans. Ind. Electron*., vol. 62, no. 9, pp. 5458–5467, Sep. 2015.

[11] J. Liu, S. Jiang, D. Cao, and F. Z. Peng, “A digital current control of quasi-Z-source inverter with battery,” *IEEE Trans. Ind. Informat.*, vol. 9, no. 2, pp. 928–937, Apr. 2013.

[12] M. Shen, A. Joseph, J. Wang, F. Z. Peng, and D. J. Adams, “Comparison of traditional inverters and Z-source inverter for fuel cell vehicles*," IEEE Trans. Power Electron*., vol. 22, no. 4, pp. 1453–1463, Jul. 2007.

[13] A. Battiston, J.-P. Martin, E.-H. Miliani, B. Nahid-Mobarakeh, S. Pierfederici, and F. Meibody-Tabar, “Comparison criteria for electric traction system using Z-source/quasi Z-source inverter and conventional architectures,” *IEEE J. Emerg. Sel. Topics Power Electron*., vol. 2, no. 3, pp. 467–476, Sep. 2014.

[14] H. Snani, M. Amarouayache, A. Bouzid, A. Lashab and H. Bounechba, "A study of dynamic behaviour performance of DC/DC boost converter used in the photovoltaic system," *2015 IEEE 15th International Conference on Environment and Electrical Engineering (EEEIC)*, Rome, 2015, pp. 1966-1971.

[15] M. Chamana, B. H. Chowdhury and F. Jahanbakhsh, "Distributed Control of Voltage Regulating Devices in the Presence of High PV Penetration to Mitigate Ramp-Rate Issues," *in IEEE Transactions on Smart Grid*, vol. 9, no. 2, pp. 1086-1095, March 2018.

[16] T. V. Thang, A. Ahmed, C. Kim and J. Park, "Flexible System Architecture of Stand-Alone PV Power Generation With Energy Storage Device," *in IEEE Transactions on Energy Conversion*, vol. 30, no. 4, pp. 1386-1396, Dec. 2015.

[17] Y. Liu, B. Ge, H. Abu-Rub and F. Z. Peng, "Control System Design of Battery-Assisted Quasi-Z-Source Inverter for Grid-Tie Photovoltaic Power Generation," *in IEEE Transactions on Sustainable Energy*, vol. 4, no. 4, pp. 994-1001, Oct. 2013.

[18] B. Ge, F. Z. Peng, H. Abu-Rub, F. J. T. E. Ferreira and A. T. de Almeida, "Novel Energy Stored Single-Stage Photovoltaic Power System With Constant DC-Link Peak Voltage*," in IEEE Transactions on Sustainable Energy*, vol. 5, no. 1, pp. 28-36, Jan. 2014.

[19] A. Lashab, D. Sera, J. Martins and J. M. Guerrero, "Model Predictive-Based Direct Battery Control in PV Fed Quasi Z-Source Inverters," 2018 5th *International Symposium on Environment-Friendly Energies and Applications* (EFEA), Rome, 2018, pp. 1-6.

[20] S. Kouro, P. Cortes, R. Vargas, U. Ammann and J. Rodriguez, "Model Predictive Control—A Simple and Powerful Method to Control Power Converters," *in IEEE Trans. on Industrial Electron.*, vol. 56, no. 6, pp. 1826-1838, June 2009.

[21] S. Bayhan, H. Abu-Rub and R. S. Balog, "Model Predictive Control of Quasi-Z-Source Four-Leg Inverter," *in IEEE Trans. on Ind. Electronics*, vol. 63, no. 7, pp. 4506-4516, July 2016.

[22] A. Lashab, A. Bouzid and H. Snani, "Comparative study of three MPPT algorithms for a photovoltaic system control," 2015 *World Congress on Information Technology and Computer Applications* (WCITCA), Hammamet, 2015, pp. 1-5. doi: 10.1109/WCITCA.2015.7367039

[23] A. Bakeer, M. A. Ismeil and M. Orabi, "A Powerful Finite Control Set-Model Predictive Control Algorithm for Quasi Z-Source Inverter," *in IEEE Transactions on Industrial Informatics*, vol. 12, no. 4, pp. 1371-1379, Aug. 2016.

[24] S. Bayhan, M. Trabelsi, H. Abu-Rub and M. Malinowski, "Finite-Control-Set Model-Predictive Control for a Quasi-Z-Source Four-Leg Inverter Under Unbalanced Load Condition," *in IEEE Transactions on Industrial Electronics*, vol. 64, no. 4, pp. 2560-2569, April 2017.

[25] M. Mosa, R. S. Balog and H. Abu-Rub, "High-Performance Predictive Control of Quasi-Impedance Source Inverter," *in IEEE Transactions on Power Electronics*, vol. 32, no. 4, pp. 3251-3262, April 2017.

[26] Y. Liu, B. Ge, H. Abu-Rub, H. Sun, F. Z. Peng and Y. Xue, "Model Predictive Direct Power Control for Active Power Decoupled Single-Phase Quasi-Z-Source Inverter," *in IEEE Transactions on Industrial Informatics*, vol. 12, no. 4, pp. 1550-1559, Aug. 2016.

[27] M. Ciobotaru, R. Teodorescu and F. Blaabjerg, "A new single-phase PLL structure based on second order generalized integrator," *37th IEEE Power Electronics Specialists Conference*, Jeju, 2006, pp. 1-6.